

## Supplementary Information

### Preorganized helical chirality controlled homochiral self-assembly and circularly polarized luminescence in a quadruple-stranded Eu<sub>2</sub>L<sub>4</sub> helicate

Guoying Han, Yanyan Zhou, Yuan Yao, Zhenyu Cheng, Ting Gao, Hongfeng Li,\* and Pengfei Yan\*

Key Laboratory of Functional Inorganic Material Chemistry, Ministry of Education, P. R. China; School of Chemistry and Materials Science, Heilongjiang University, Harbin 150080, P. R. China.

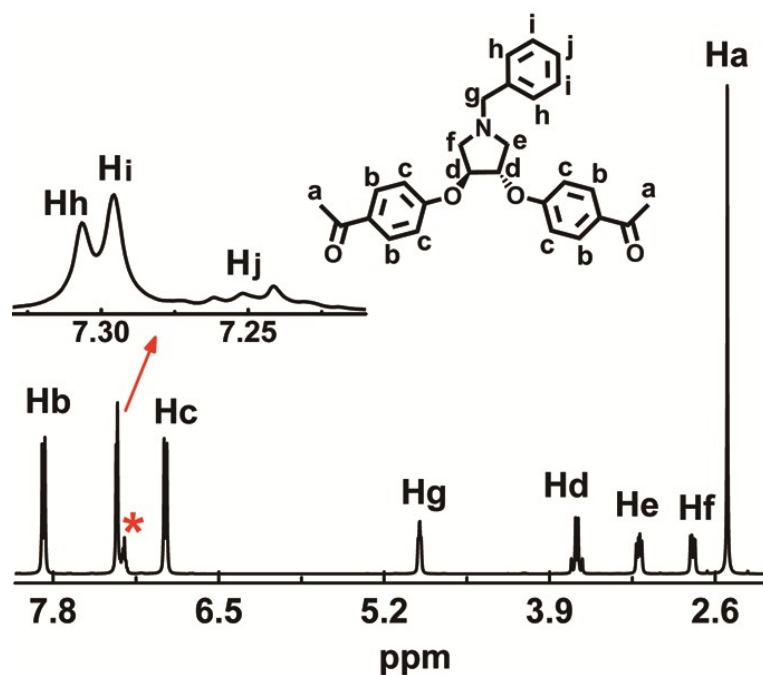


Figure S1. <sup>1</sup>H NMR spectrum of (S,S)-4a in CDCl<sub>3</sub>.

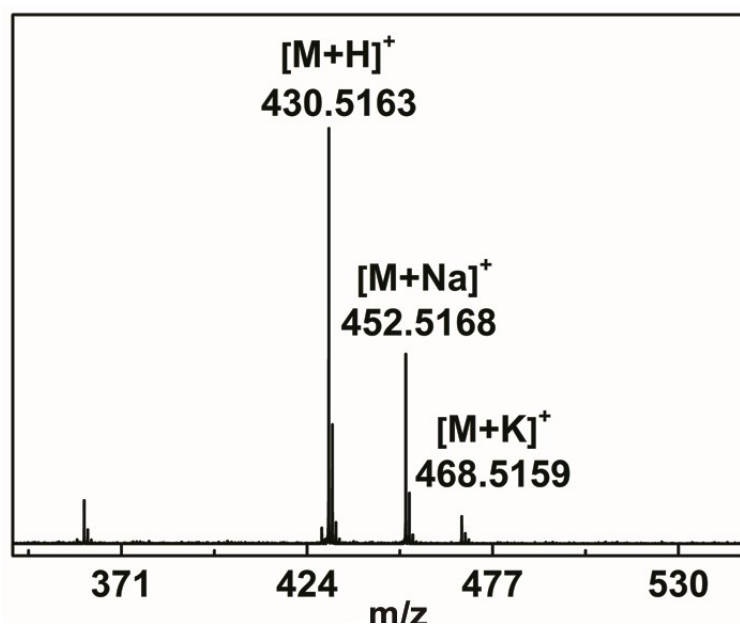


Figure S2. ESI-TOF-MS of (S,S)-4a.

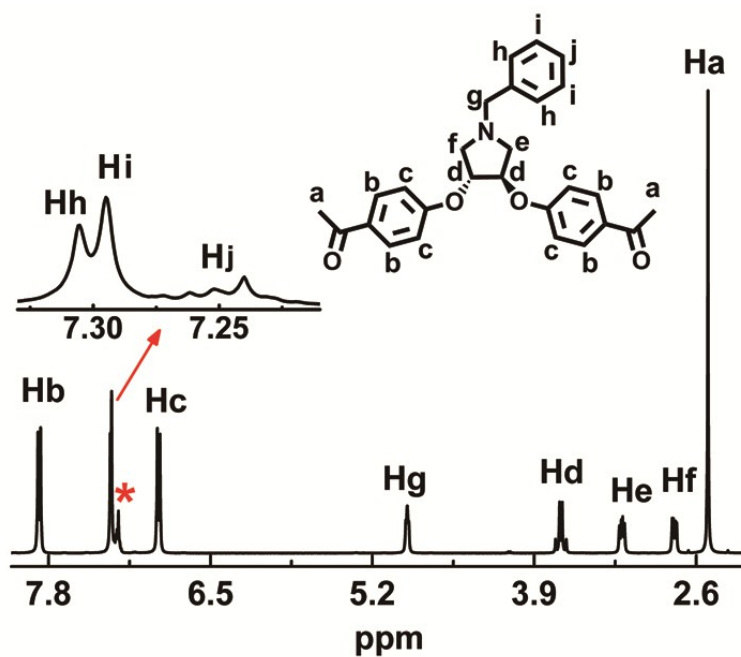


Figure S3. <sup>1</sup>H NMR spectrum of (R,R)-4a in CDCl<sub>3</sub>.

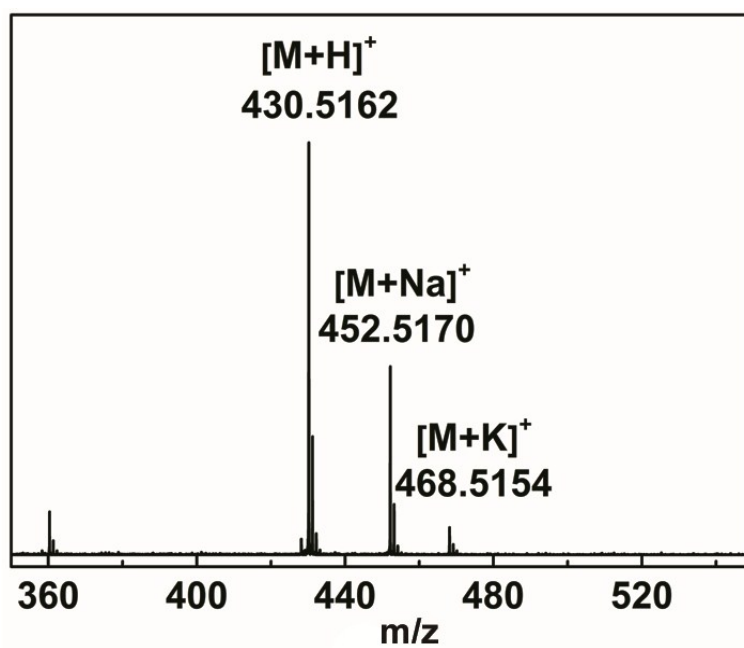


Figure S4. ESI-TOF-MS of (R,R)-4a.

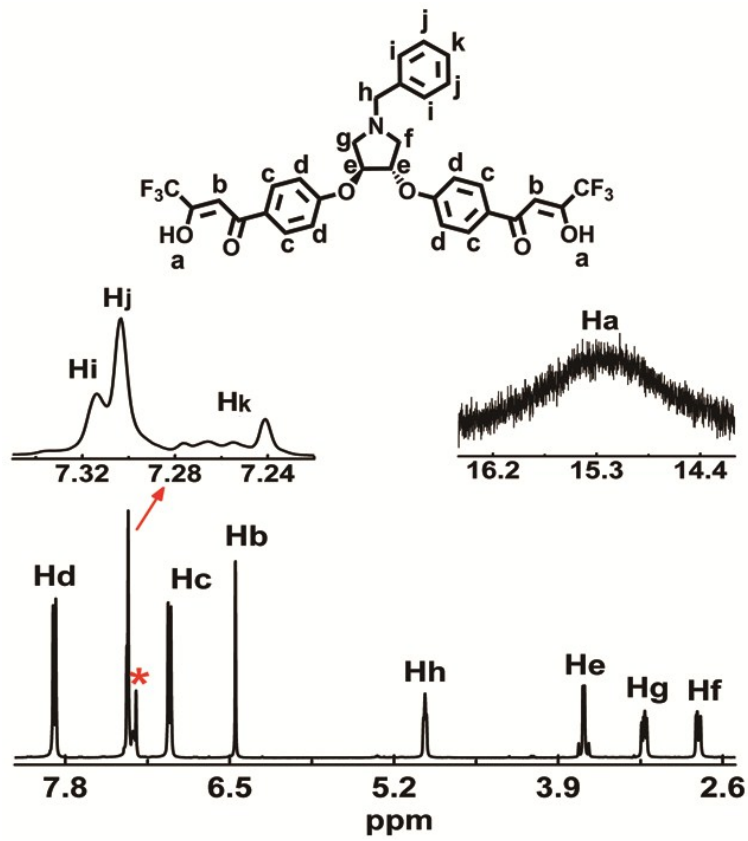


Figure S5. <sup>1</sup>H NMR spectrum of **L<sup>SS</sup>** in CDCl<sub>3</sub>.

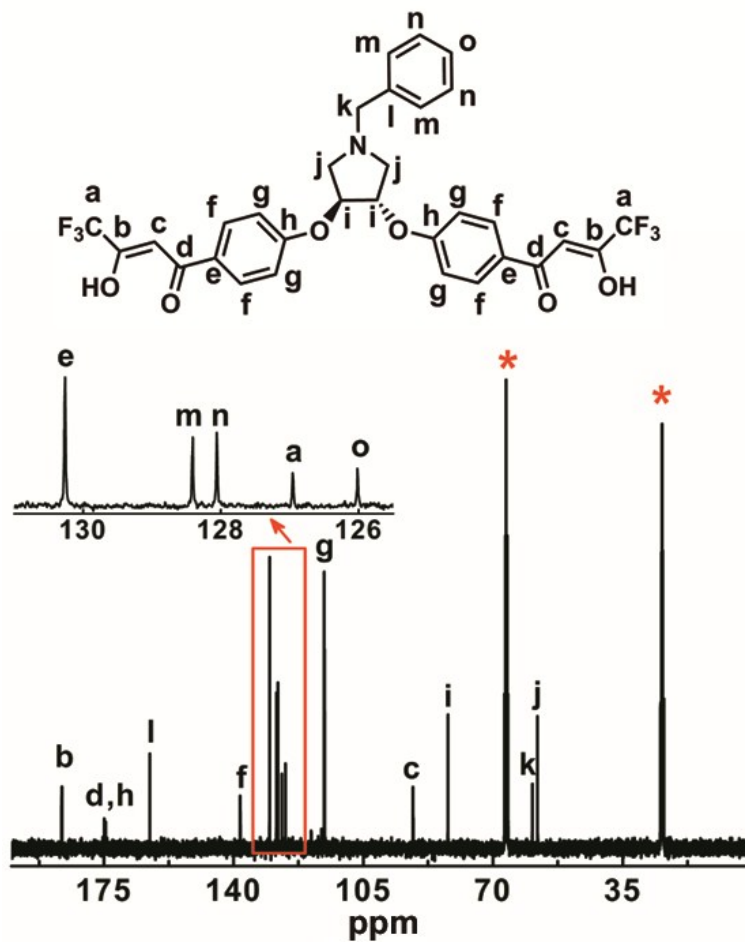


Figure S6.  $^{13}C$  NMR spectrum of  $L^{SS}$  in THF- $d_8$ .

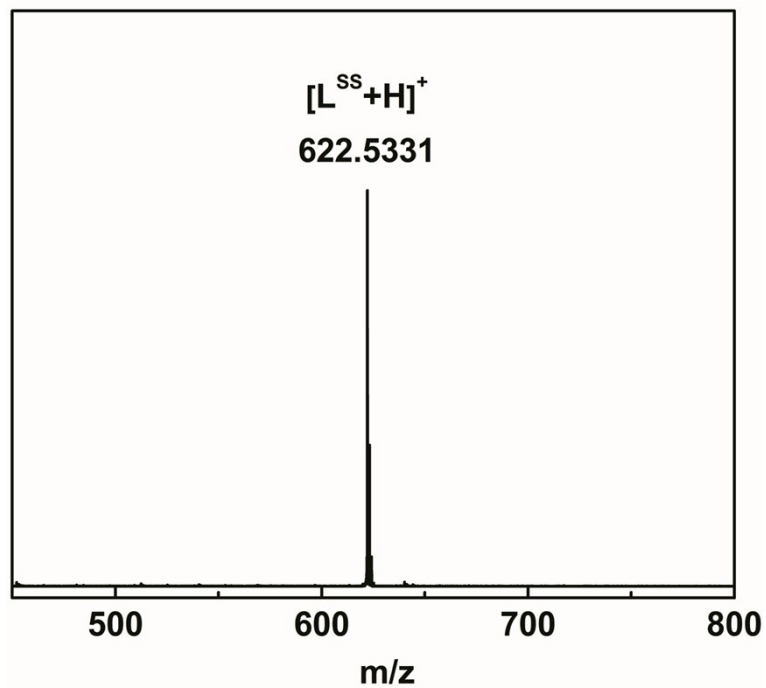


Figure S7. ESI-TOF-MS of  $L^{SS}$ .

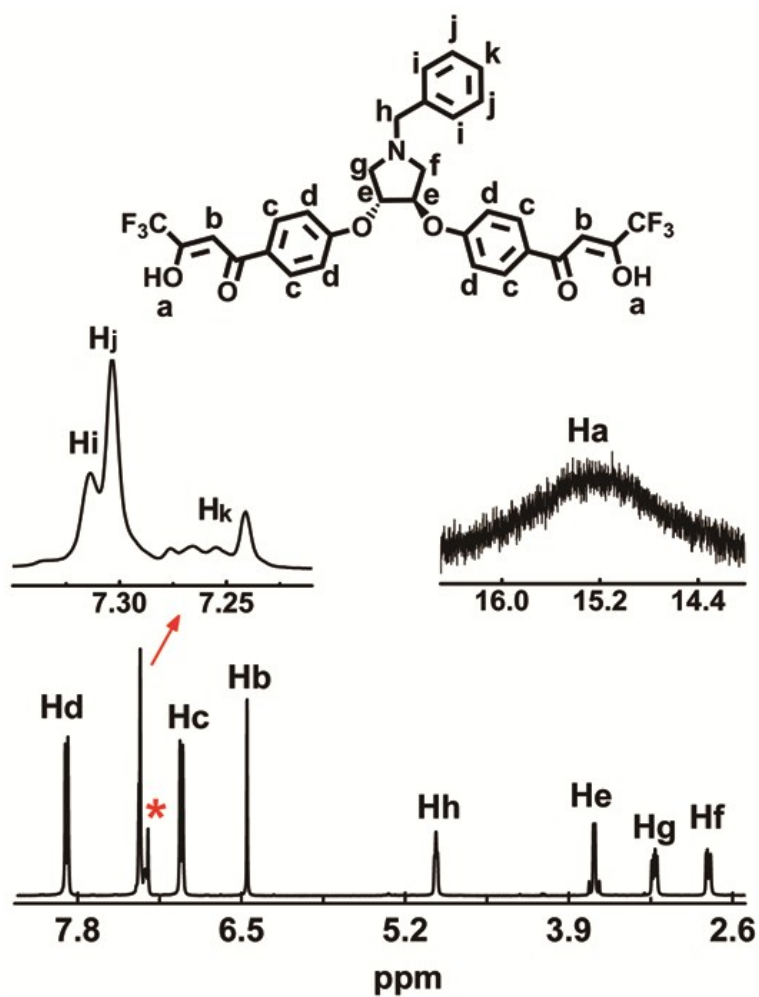


Figure S8.  $^1H$  NMR spectrum of  $L^{RR}$  in  $CDCl_3$ .

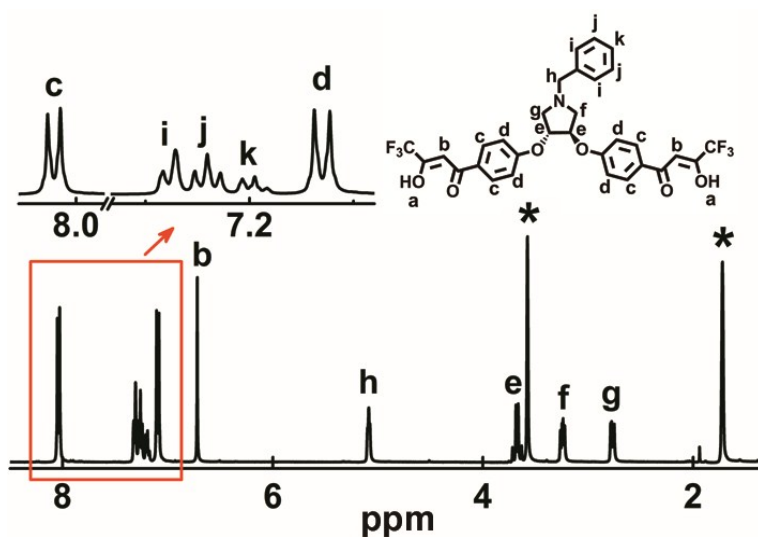


Figure S9.  $^1H$  NMR spectrum of  $L^{RR}$  in  $THF-d_8$ .

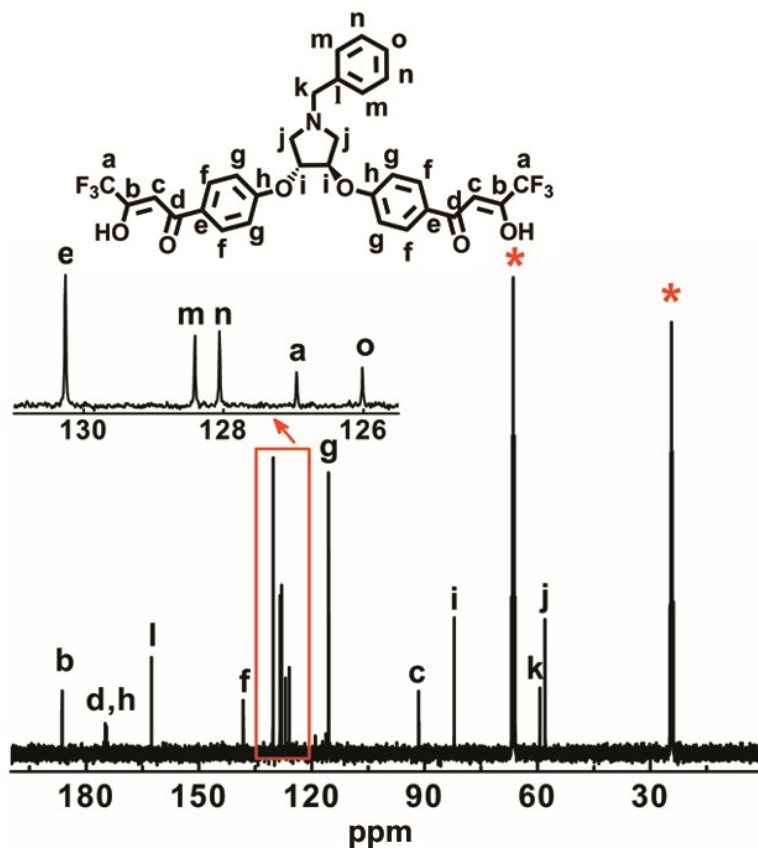


Figure S10.  $^{13}\text{C}$  NMR spectrum of  $L^{RR}$  in  $\text{THF-}d_8$ .

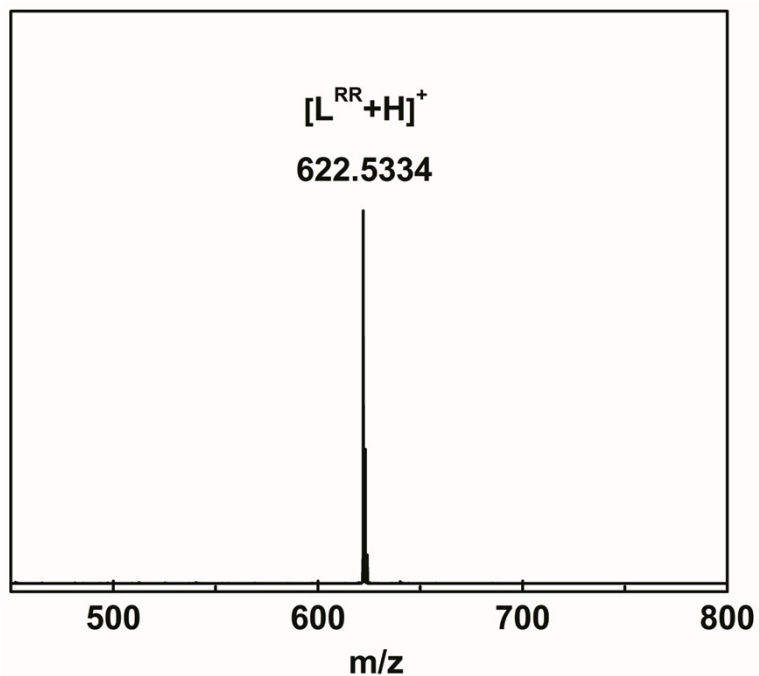


Figure S11. ESI-TOF-MS of  $L^{RR}$ .

**Table S1. Crystal data of the ligands L<sup>SS</sup> and L<sup>RR</sup>.**

	L <sup>SS</sup>	L <sup>RR</sup>
CCDC Number	1972802	1972801
formula	C <sub>31</sub> H <sub>25</sub> F <sub>6</sub> N O <sub>6</sub>	C <sub>31</sub> H <sub>25</sub> F <sub>6</sub> N O <sub>6</sub>
Mr	621.52	621.52
cryst syst	orthorhombic	orthorhombic
space group	<i>P</i> 2 <sub>1</sub> 2 <sub>1</sub> 2 <sub>1</sub>	<i>P</i> 2 <sub>1</sub> 2 <sub>1</sub> 2 <sub>1</sub>
<i>a</i> (Å)	9.103(5)	9.105(5)
<i>b</i> (Å)	11.578(5)	11.571(5)
<i>c</i> (Å)	27.425(5)	27.397(5)
<i>α</i> (deg)	90	90
<i>β</i> (deg)	90	90
<i>γ</i> (deg)	90	90
<i>V</i> (Å <sup>3</sup> )	2890(2)	2886(2)
<i>Z</i>	4	4
<i>ρ</i> (g cm <sup>3</sup> )	1.424	1.430
<i>μ</i> (mm <sup>-1</sup> )	0.124	0.124
<i>F</i> (000)	1272.0	1280.0
<i>R</i> <sub>1</sub> , [ <i>I</i> > 2σ( <i>I</i> )]	0.0600	0.0608
<i>wR</i> <sub>2</sub> , [ <i>I</i> > 2σ( <i>I</i> )]	0.1513	0.1594
<i>R</i> <sub>1</sub> , (all data)	0.1087	0.0987
<i>wR</i> <sub>2</sub> , (all data)	0.1888	0.1962
GOF on <i>F</i> <sup>2</sup>	1.022	1.049

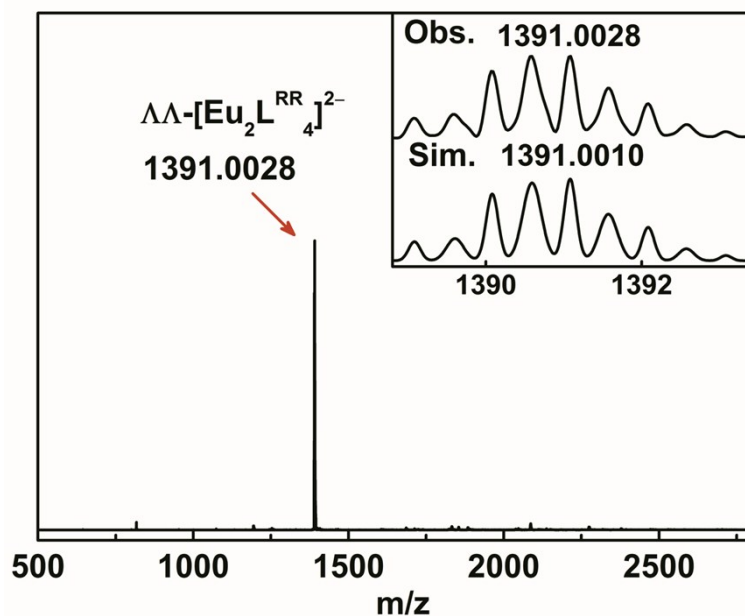


Figure S12. ESI-TOF-MS of  $\Delta\Delta\text{-}(\text{Eu}_2\text{L}^{\text{RR}}_4)^{2-}$ .

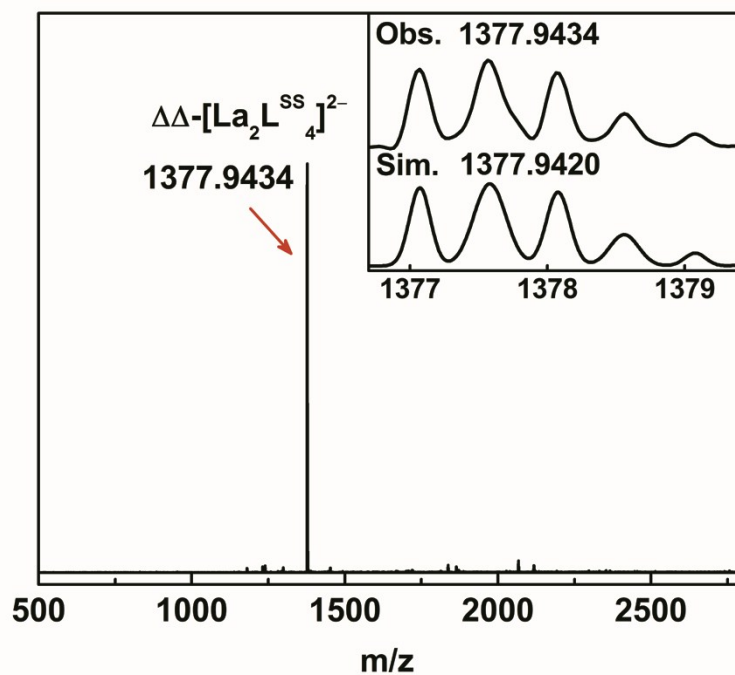


Figure S13. ESI-TOF-MS of  $\Delta\Delta\text{-}(\text{La}_2\text{L}^{\text{SS}}_4)^{2-}$ .



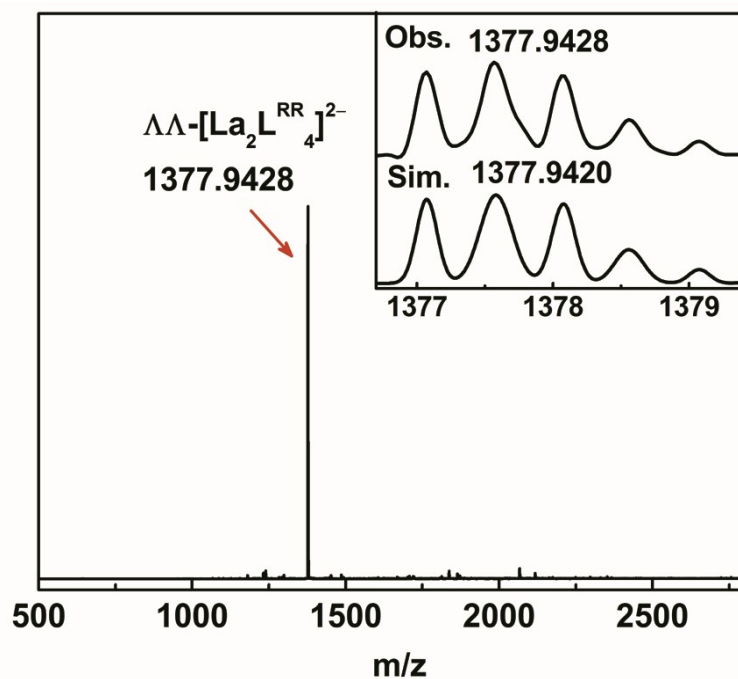


Figure S14. ESI-TOF-MS of  $\Delta\Delta\text{-}(\text{La}_2\text{L}^{\text{RR}}_4)^{2-}$ .

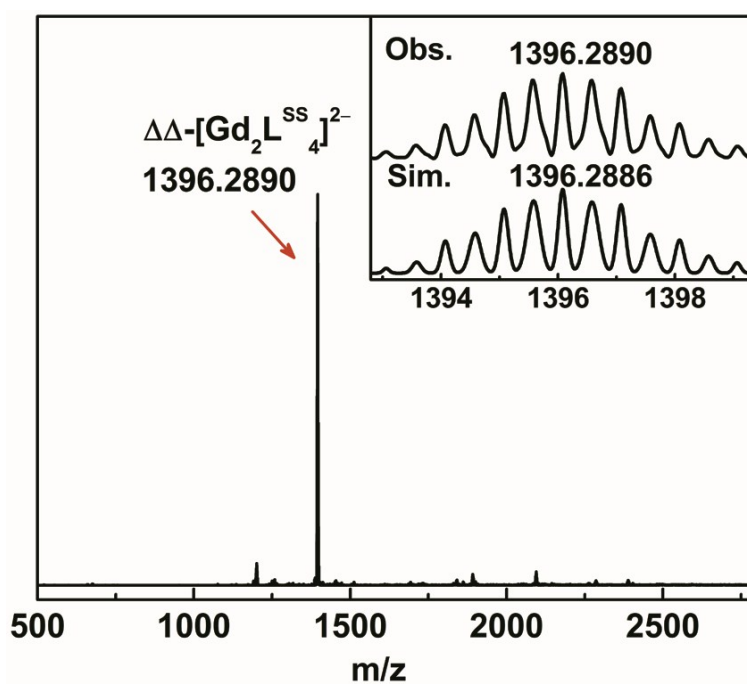


Figure S15. ESI-TOF-MS of  $\Delta\Delta\text{-}(\text{Gd}_2\text{L}^{\text{SS}}_4)^{2-}$ .

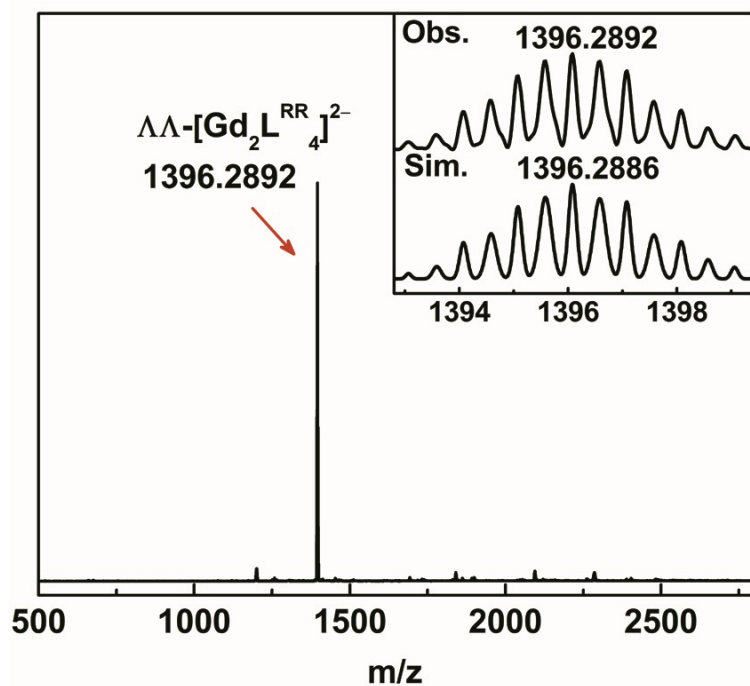


Figure S16. ESI-TOF-MS of  $\Delta\Delta\text{-}(\text{Gd}_2\text{L}^{\text{RR}}_4)^{2-}$ .

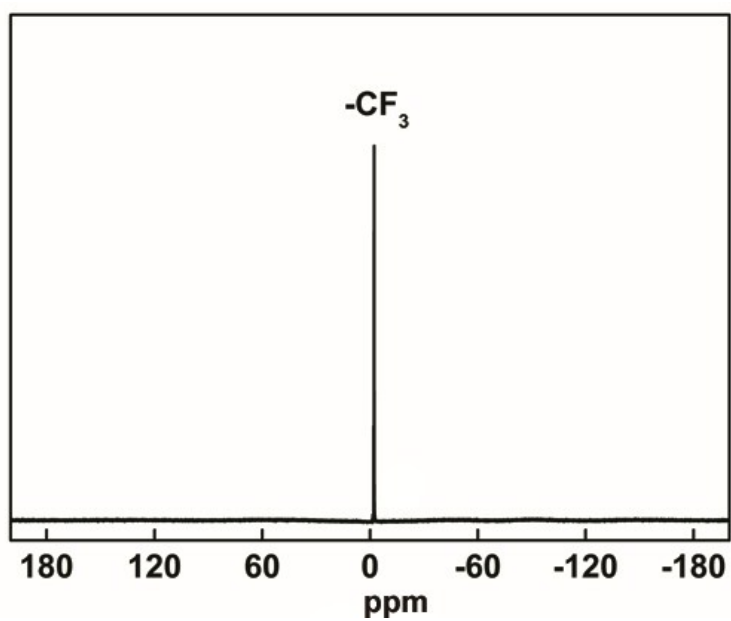


Figure S17.  $^{19}\text{F}$  NMR spectrum of  $\Delta\Delta\text{-}(\text{HNEt}_3)_2(\text{Eu}_2\text{L}^{\text{SS}}_4)$  in  $\text{THF-}d_8$ .

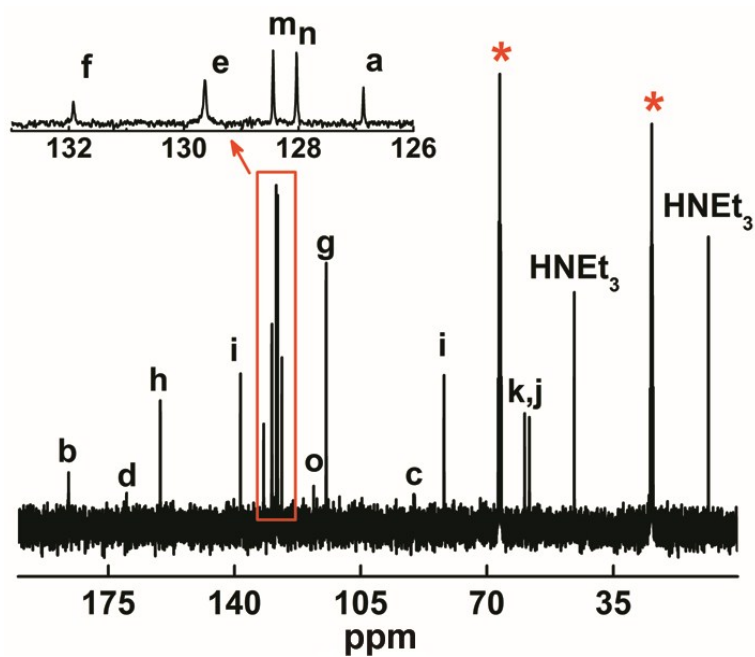


Figure S18.  $^{13}\text{C}$  NMR spectrum of  $\Delta\Delta$ -( $\text{HNEt}_3$ ) $_2$ ( $\text{La}_2\text{L}^{\text{SS}}_4$ ) in  $\text{THF-}d_8$ .

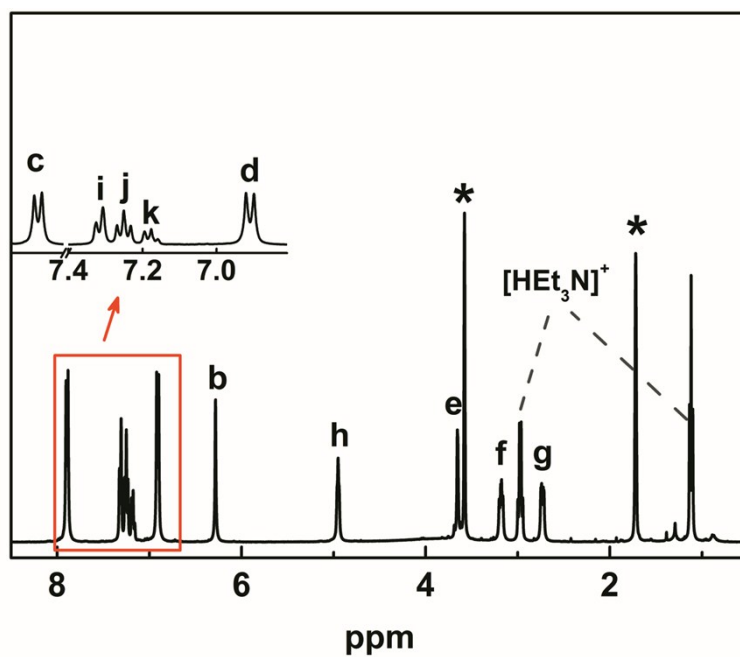


Figure S19.  $^1\text{H}$  NMR spectrum of  $\Lambda\Lambda$ -( $\text{HNEt}_3$ ) $_2$ ( $\text{La}_2\text{L}^{\text{RR}}_4$ ) in  $\text{THF-}d_8$ .

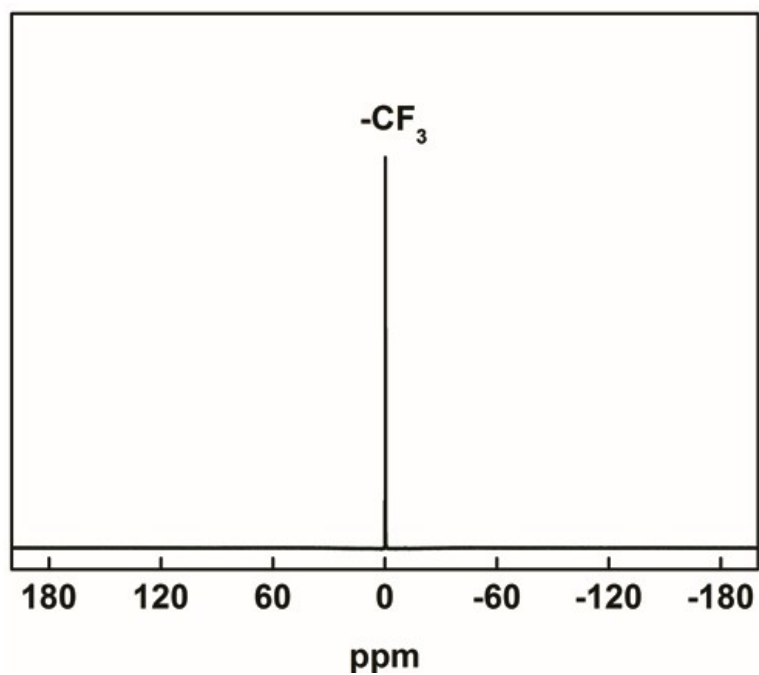


Figure S20.  $^{19}\text{F}$  NMR spectrum of  $\Lambda\Lambda\text{-(HNEt}_3)_2(\text{La}_2\text{L}^{\text{RR}_4})$  in  $\text{THF-}d_8$ .

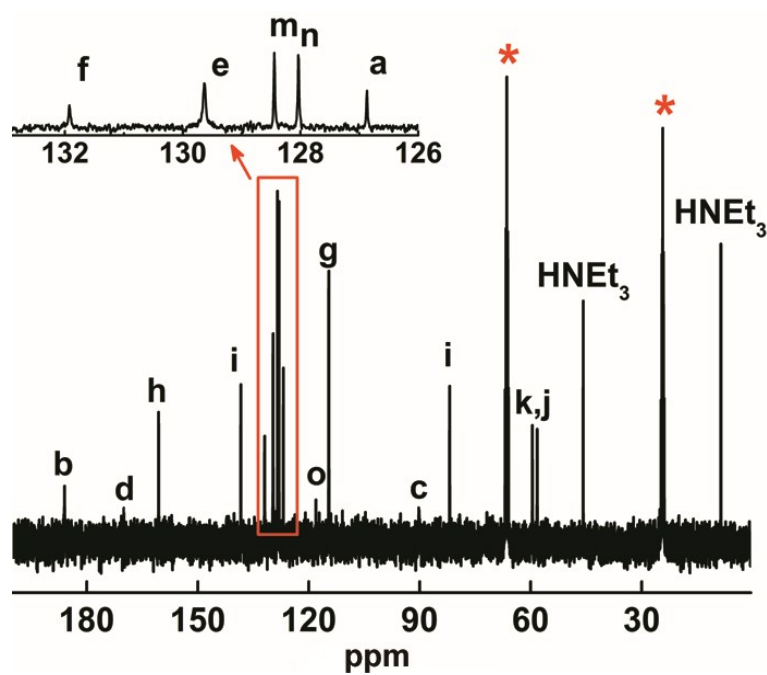
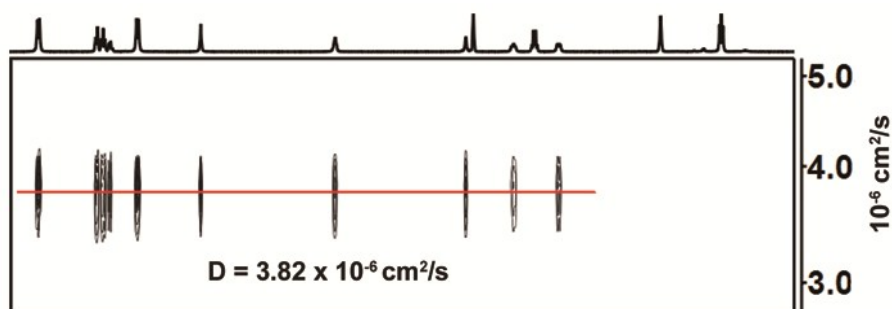
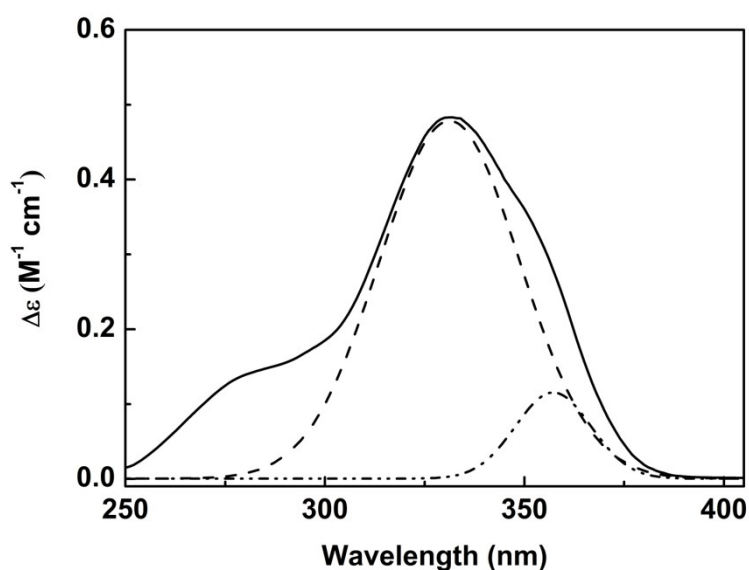


Figure S21.  $^{13}\text{C}$  NMR spectrum of  $\Lambda\Lambda\text{-(HNEt}_3)_2(\text{La}_2\text{L}^{\text{RR}_4})$  in  $\text{THF-}d_8$ .



**Figure S22.**  $^1\text{H}$  DOSY spectrum of  $\Delta\Delta\text{-(HNEt}_3)_2\text{(La}_2\text{L}^{\text{RR}}_4)$  in  $\text{THF-}d_3$ .



**Figure S23.** The experimental absorption spectrum of  $\Delta\Delta\text{-Eu}_2\text{L}^{\text{SS}}_4$  (solid line) and the deconvoluted Gaussian curves (dashed lines) that correspond to transitions to two excitonic states.

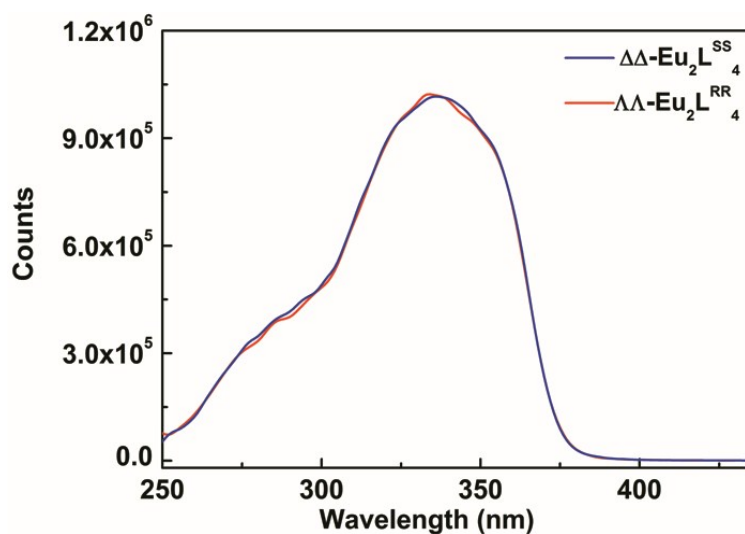


**Figure S24.** Excitation spectra of  $\Delta\Delta\text{-Eu}_2\text{L}^{\text{SS}}_4$  (blue line) and  $\Delta\Delta\text{-Eu}_2\text{L}^{\text{RR}}_4$  (red line) recorded by monitoring the emission band of  $\text{Eu}^{3+}$  ions at 613 nm in THF ( $1.0 \times 10^{-5}$  M).

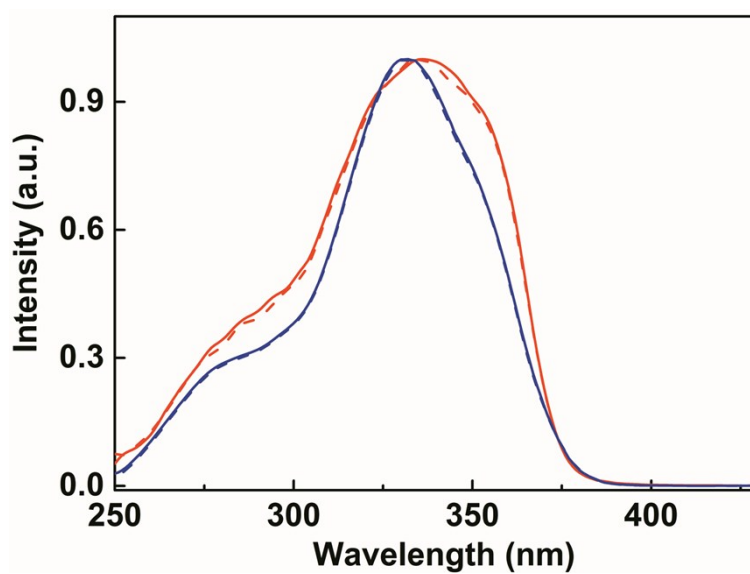


**Figure S25.** Normalization absorption (blue line,  $2.5 \times 10^{-6}$  M) and excitation spectra (red line,  $1.0 \times 10^{-5}$  M) of helicates in THF.

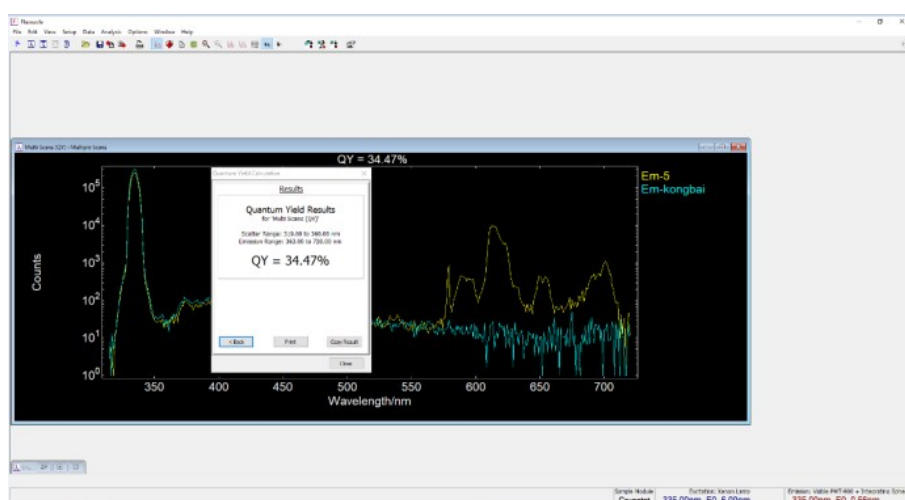


**Figure S26.** The screenshot of the luminescence quantum yield measurement of  $\Delta\Delta$ -Eu<sub>2</sub>L<sup>SS</sup><sub>4</sub>.

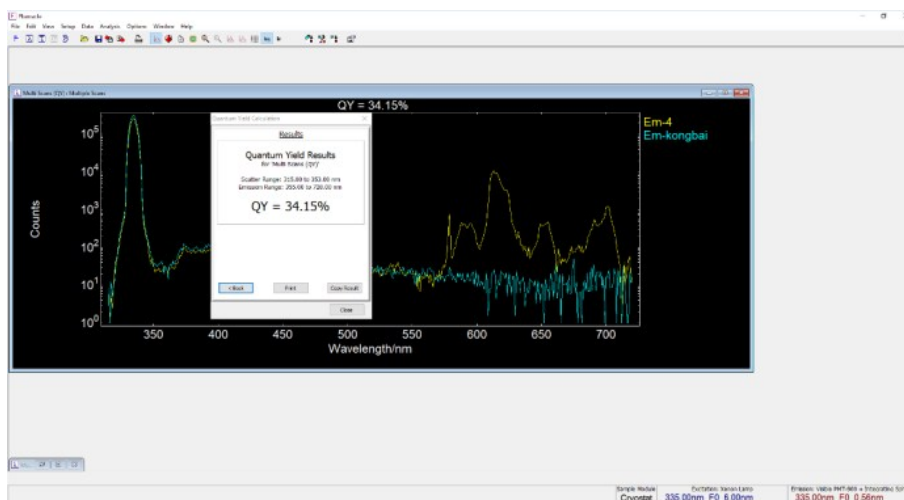


**Figure S27.** The screenshot of the luminescence quantum yield measurement of  $\Lambda\Lambda$ -Eu<sub>2</sub>L<sup>RR</sup><sub>4</sub>.

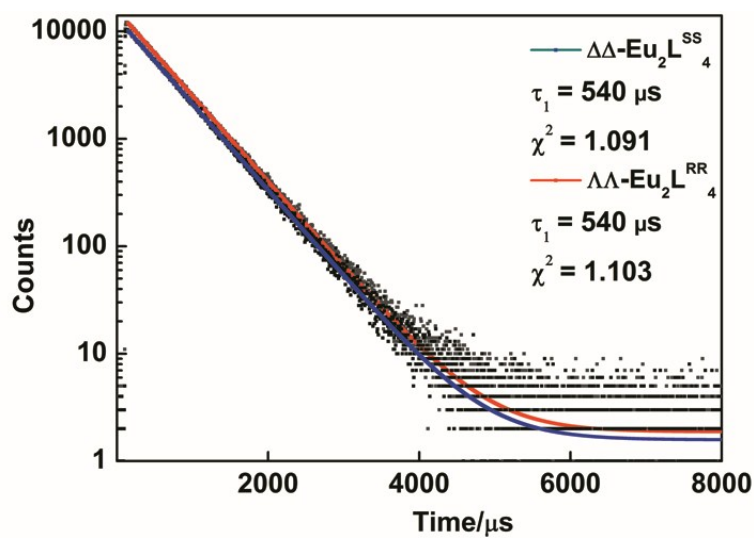


**Figure S28.** Luminescence decay curves of  $\Delta\Delta$ -Eu<sub>2</sub>L<sup>SS</sup><sub>4</sub> (blue line) and  $\Lambda\Lambda$ -Eu<sub>2</sub>L<sup>RR</sup><sub>4</sub> (red line) in THF monitored at 613nm.

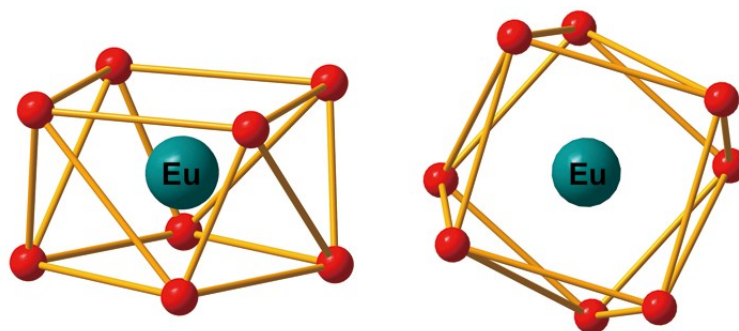


**Figure S29.** Side view (left) and top view (right) of the coordination polyhedra of  $\Delta\Delta$ -Eu<sub>2</sub>L<sup>SS</sup><sub>4</sub>.

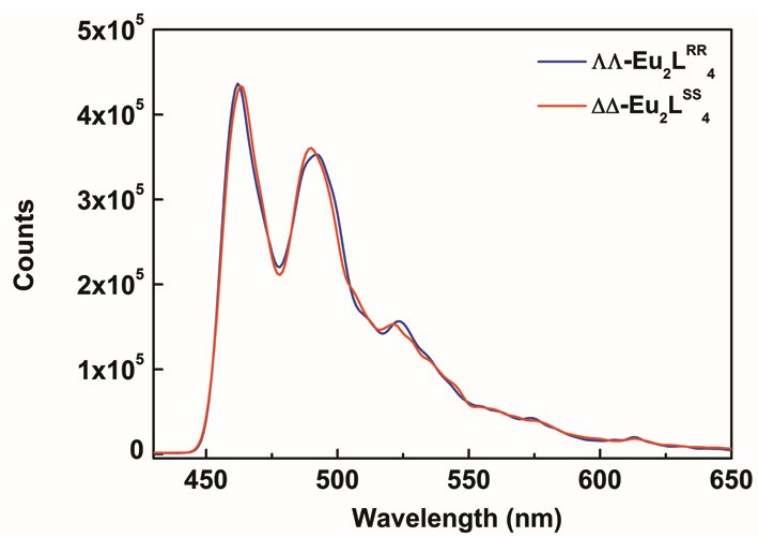


**Figure S30.** Phosphorescence spectra of  $\Delta\Delta\text{-Eu}_2\text{L}^{\text{SS}}_4$  (red line) and  $\Lambda\Lambda\text{-Eu}_2\text{L}^{\text{RR}}_4$  (blue line) in THF at 77 K.